University of Maribor Press

# Rockerbot: Rover Kinematics for Maize Farming

Matteo ZINZANI, Mirko USUELLI*, Paolo CUDRANO, Simone MENTASTI, Carlo ARNONE, Andrea CERUTTI,

Alba LO GRASSO, Abdelrahman Tarek FARAG, Matteo MATTEUCCI

Department of Electronics Information and Bioengineering, Politecnico di Milano,

Piazza Leonardo da Vinci 32, Milan, Italy

## ABSTRACT

Crop inspection plays a significant role in modern agricultural practices as it enables farmers to evaluate the condition of their fields and make informed decisions regarding crop management. However, existing methods of crop inspection are often labor-intensive, leading to slow and costly processes. Therefore, there is a pressing need for more efficient and cost-effective approaches to crop inspection to improve agricultural productivity, sustainability, and to deal with labor shortage. In this study, we present Rockerbot, a novel agricultural robot designed as a compact rover capable of navigating and surveying maize fields in their early growth stages. This technology is essential for timely landscape adjustments to ensure optimal crop production. The document offers a comprehensive review of the decisions made during the hardware and software development stages. The hardware section is centered around design choices influenced by the rover's kinematics, while the software section outlines the tasks that Rockerbot can perform using mobile perception, such as mapping, sensing, and detection.

Keywords: agricultural robotics, smart agriculture, autonomous navigation, watering, mapping

## INTRODUCTION

The rapid growth of the global population and the challenges posed by climate change have placed immense pressure on the agricultural sector to meet the increasing demand for food while minimizing environmental impacts. Among various crops, maize stands out as one of the most extensively cultivated crops worldwide, serving as a staple food source for millions of people (Statista, 2021; Erenstein et al., 2022). Addressing the need for enhanced agricultural productivity and sustainability in maize farming has become crucial, and the integration of robotics has emerged as a promising solution.

Advancements in robotics technology have opened up new possibilities for transforming traditional farming practices (Sparrow and Howard, 2021). With the ability to perform repetitive and labor-intensive tasks with precision and efficiency, robots offer significant potential for revolutionizing agriculture. Autonomous navigation, particularly in wide-ranging maize fields, has become a focal point for research and development, as it promises to automate the sector and improve overall productivity.

The automation of maize farming through the deployment of robotics allows for several key advantages.

Firstly, the introduction of autonomous navigation systems in vast agricultural areas enables robots to efficiently traverse and survey the fields, ensuring comprehensive coverage and data collection. This capability facilitates the implementation of site-specific management strategies, leading to optimized resource utilization and improved crop health. Furthermore, due to global warming posing new challenges for maize pest control (Diffenbaugh et al., 2008), existing farming practices will be intensely scrutinized year after year. Automation undoubtedly contributes to the enhancement of autonomous analysis. Secondly, the need for automation in agriculture is driven by the swift expansion of the global population. This growth is creating an exponential demand for food that our current land resources are struggling to meet (Ritson, 2020).

### Related Works

Autonomous navigation in crop fields is an emerging area of study, and the current state-of-the- art offers limited solutions for effectively accomplishing this task. The existing literature primarily focuses on either the vision or point cloud domain in terms of perception.

Real-Time Kinematic (RTK) and Differential Global

Positioning System (DGPS) are advanced techniques used to enhance the accuracy of location data from satellite-based positioning systems like GPS (Global Positioning System). RTK is a type of DGPS that uses a newer technology and protocol for more precise measurements. RTK-DGPS relies on signals from satellites to perform triangulation, a process where it measures the distances between you and at least four satellites to calculate your precise location on Earth. (Bakker et al., 2010) introduced an early method for autonomous maize navigation using RTK-DGPS technology to navigate the maize fields. This information provides coordinates, such as latitude and longitude, facilitating accurate navigation regardless of external landmarks. The initial trajectory is established by recording the first line formed by the edge point A-B. Subsequently, a complete parallel trajectory to the initial segment A-B is generated for navigation purposes. It is important to note that this route plan does not account for headlands and requires prior information about field boundaries, specifically at certain points. However, since RTK-DGPS is not universally accessible, alternative navigation systems independent of RTK-DGPS began to be explored within the research community, aiming to provide reliable positioning solutions in scenarios where RTK-DGPS signals may be limited or denied, particularly in remote or densely vegetated agricultural areas.

In the agricultural sector, particularly in crop fields, vision-based systems are favored due to their cost-effectiveness when compared to LiDARs and radars. The employment of vision-based systems has been extensively suggested as a potential solution for this task (Yang et al., 2018; Chen et al., 2020; Liu et al., 2016). (Yang et al., 2018) presented a vision system capable of filtering images based on the red color to detect the visible roots of maize plants. This detection was then refined using the least square method to determine the optimal path to be followed. In a similar vein, (Chen et al., 2020) proposed an alternative approach by employing the Hough transformation to identify the central navigation line. Another variation was introduced by (Liu et al., 2016), who developed a monocular vision navigation system for maize canopy based on RBF (Radial Basis Function). This method, unlike the least square and Hough transformation techniques, exhibited better handling of line following in the presence of curvature. However, it is worth noting that all of these methods have been specifically tuned for a particular life stage cycle of maize.

Indeed, LiDAR-based systems have been developed to account for the changes that occur throughout the life cycle of plants. (Reiser et al., 2016) demonstrated the feasibility of offline route planning by utilizing laser scan data collection paired with RANSAC fitting (Fischler and Bolles, 1981).

Nevertheless, their research was limited to greenhouse settings, and real-time performance is not guaranteed as no further data processing was performed. In contrast, (Hiremath et al., 2014) proposed a probabilistic model based on a particle filter, using a 2D LiDAR sensor. This approach showcased promising performance across different conditions, as it was specifically designed to address uncertainties, although the same particle filter approach applied to the 3D LiDAR point cloud could suffer computational complexity.

Previous research (Cudrano et al., 2022) has demonstrated that the process of autonomous navigation in agricultural fields can be divided into two main stages: navigating through rows and executing turns. The stage of row navigation employs 2D LiDAR scans and clustering algorithms to distinguish between crop rows. The detection of the end of a row triggers the transition to the turning stage. During this stage, the ROS (Robot Operating System) navigation stack and SLAM (Simultaneous Localization and Mapping) work together to generate a laser-based map, which aids in planning and localization. The two-stage process emphasizes the importance of identifying the end of a row for spatial perception and turn planning. Recognizing the row's end is crucial, informing spatial understanding and enabling effective turning strategies, thereby enhancing overall navigation efficiency in agricultural settings.

## Proposal

This study builds upon our prior work (Cudrano et al., 2022) and introduces a novel robotic platform, Rockerbot, specifically engineered for autonomous farming tasks in maize fields (Fig. 1). The main role of our system is to autonomously navigate through maize rows that are 0.70 – 0.75m wide. Rockerbot's ability to execute complex maneuvers, such as navigating around obstacles with accurate turns, is dependent on its mapping capabilities, which are facilitated by LiDAR sensors. In addition to its primary navigation tasks, Rockerbot is also equipped to detect objects and simultaneously irrigate side crops.



**Figure 1:** Rockerbot navigating through a maze field

## MATERIAL AND METHODS

The goal of the designed robot is to perform diverse tasks in an agricultural field, specifically a maize field. The critical parameters of this scenario include plant height ($0.3m$ - $0.4m$), row- to-row spacing of $0.70 – 0.75m$, and predominantly flat but well-drained terrain with minor irregularities. The robot is designed to have autonomous navigation capabilities, precisely moving between maize rows without inflicting damage, detecting obstacles, and identifying various objects. Additionally, it should provide flexibility by facilitating the attachment of different tools like additional and specialized cameras, small robotics arms, and spraying systems to enhance task diversity.

The locomotion and kinematics of the robot, shown in Fig. 2, have been chosen after an accurate analysis of the state of the art (Rubio et al., 2019) and taking into account the operating environment.
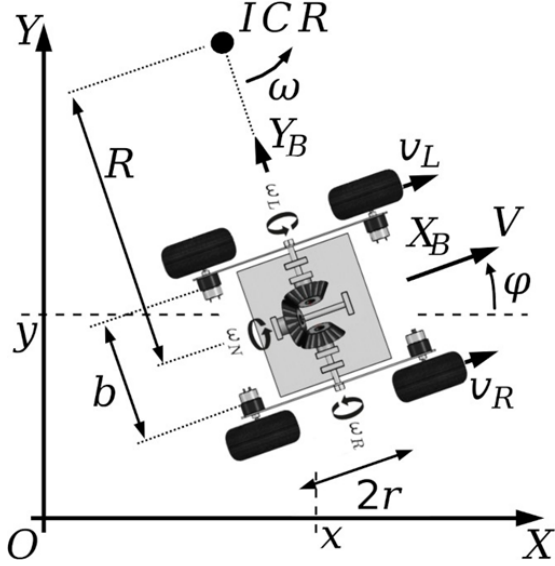


**Figure 2:** Kinematic scheme of Rockerbot with its bevel gear suspension system

For simplicity and adaptability, a wheeled system was chosen, as opposed to legged robots. Several factors influenced the design decisions, such as field dimensions, terrain requirements, power distribution, and stability. The selected design consists of a robot with a $0.4m$ width, in-hub motorized wheels for even power distribution, and a four-wheel design to enhance weight distribution and ground contact area. These decisions ensure greater stability and reduce the likelihood of rollover due to irregular terrain.

The robot incorporates a bevel gear suspension system, enabling smooth movement and facilitating cleaner data acquisition from onboard sensors by minimizing terrain-induced vibrations. This suspension system allows for the replication of movement from one side of the robot to the opposite side, thereby evenly distributing torque and

smoothing out the effects of terrain irregularities. Furthermore, a skid-steering mechanism was integrated into the robot's steering system, preserving both construction simplicity (Kozłowski and Pazderski, 2004) and the overall robustness of the system. The direct kinematics of this robot remain similar to a differential drive (Wang et al., 2015), where the primary difference lies in the baseline, which depends on wheel slippage rather than the actual distance between the wheels. These particular design choices enable the robot's effective operation within the agricultural environment, demonstrating the potential to handle various tasks efficiently and effectively.
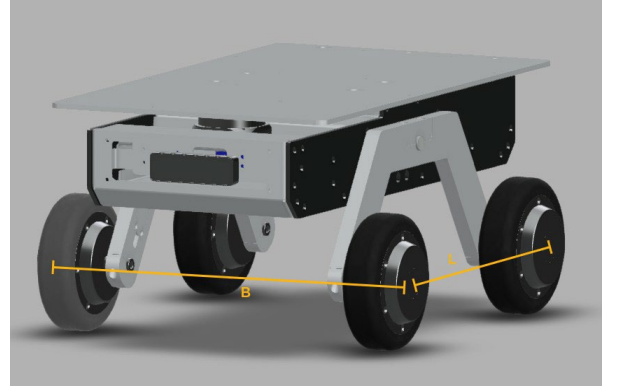


**Figure 3a:** Rockerbot's chassis and dimensions for wheel placement



**Figure 3b:** Suspension system with a single- wheel bump



**Figure 3c.** Deployment of Rockerbot in a Real- World Cornfield

**Figure 3:** Perspectives collection of Rockerbot's design

In Fig. 3, it is possible to see the compact chassis of Rockebot (Fig. 3a), along with its mechanism for averaging out irregularities in ground conditions either in testing conditions (Fig. 3b) or in real scenarios (Fig. 3c).

## Kinematic model

The kinematics of the proposed robot adhere to a skid-steering model and incorporate a distinctive feature known as the *Averaging Mechanism*. This mechanism serves to dampen ground shocks by maintaining equilibrium in the pitch angle between the right and left wheel pairs. While bearing similarities to the 'Rocker-Bogie Suspension System' introduced in the literature by NASA in 1988, our kinematics presents a simplified iteration with four wheels, as opposed to the original six-wheel design.

Skid-steering robots are vehicles that use differential steering for motion control. They have two wheels or tracks, each independently driven by its motor. The kinematic equations for a skid-steering robot describe how its position and orientation change over time based on the inputs to the two wheels or tracks. Here are the basic kinematic equations for such a robot:

Let:
- $v$ be the linear velocity of the robot (speed along a straight line).
- $\omega$ be the angular velocity of the robot (rate of rotation).
- $L$ be the distance between the two wheels or tracks (the wheelbase).
- $R$ be the radius of the wheels.

The kinematic equations are as follows:

1.   Linear Velocity ($v$):

$$V = \frac{R}{2} \cdot (\omega_r + \omega_l) \tag{1}$$

where $\omega_r$ and $\omega_l$ are the angular velocities of the left and right wheels, respectively.

2.   Angular Velocity ($\omega$):

$$V = \frac{R}{L} \cdot (\omega_r + \omega_l) \tag{2}$$

where $\omega_r$ and $\omega_l$ are the angular velocities of the left and right wheels, respectively.

3.   Robot's Position Update: The robot's position can be updated using the following Euler integration, assuming that $\theta$ is the current orientation angle of the robot:

$$x_{new} = x_{old} + V \cdot \cos(\theta) \cdot \Delta t, \tag{3}$$
$$y_{new} = y_{old} + V \cdot \sin(\theta) \cdot \Delta t, \tag{4}$$

$$\theta_{new} = \theta_{old} + \omega \cdot \Delta t, \tag{5}$$
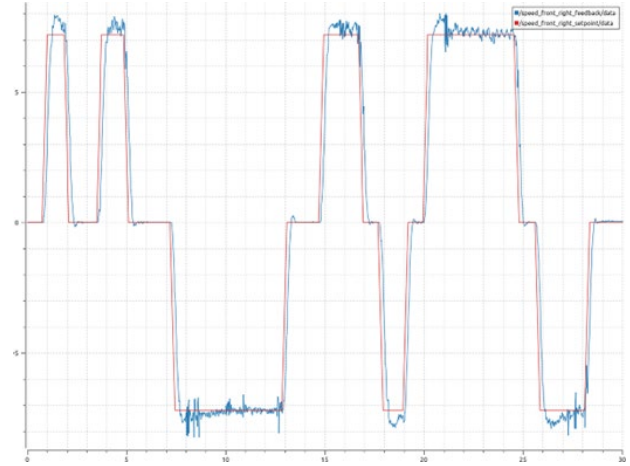
where $\Delta t$ is the time step between updates.



**Figure 4a:** PID control input sequence where the red line is the command value to be followed, and the blue one is the robot's response
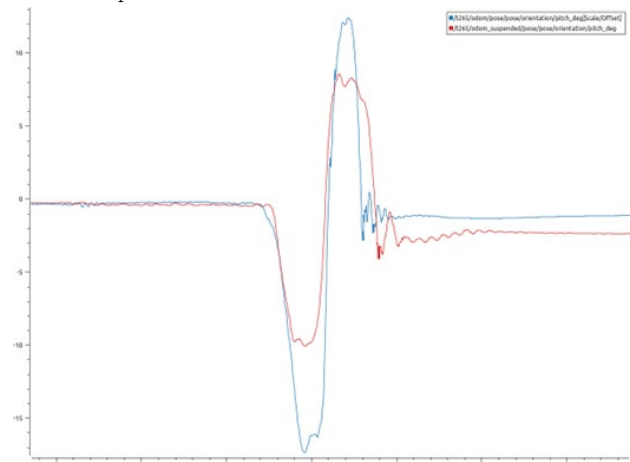


**Figure 4b:** Bump test comparison in stability with (red line) and without (blue line) active suspension system for soil irregularities

**Figure 4:** The design decisions for the Rockerbot are illustrated in the accompanying diagrams

The equations in question delineate the relationship between a skid-steering robot's linear and angular velocities and the wheel velocities ($\omega_r$ and $\omega_l$). Furthermore, they illustrate how its position and orientation change over time based on these velocities. This mathematical model plays a pivotal role in programming the robot's motion control and carrying out tasks such as path following and odometry. To ensure motion stability with the command input $[v, \omega]^T$, we fine-tuned a PID controller empirically. The optimal values obtained were $P = 0.02$, $I = 0.8$, $D = 0$, as depicted in Fig. 4a by comparing the command value to Rockerbot's response to the input.

## Bevel gear suspension system

The angular velocity of a bevel gear suspension system can be determined using the principles of rotational motion. Bevel gears are used to transmit motion between non-parallel shafts, and the angular velocity relationship for such a system can be described using the gear ratio.

If we consider a setup where one bevel gear is located on the input shaft and the other on the output shaft, we can use a specific equation to determine the relationship between the angular velocity of the input gear and that of the output gear:

$$N_{in} \cdot \omega_{in} = N_{out} \cdot \omega_{out}, \tag{6}$$

where:

- $N_{in}$ denotes the number of teeth present on the input bevel gear.
- $\omega_{in}$ signifies the angular velocity of the input shaft, measured in radians per second.
- $N_{out}$ represents the number of teeth on the output bevel gear.
- $\omega_{out}$ represents the angular velocity of the output shaft, measured in radians per second.

Equation 6 is rooted in the principle of angular momentum conservation, which asserts that the product of the number of teeth and the angular velocity remains constant when gears are engaged with each other.

To determine either the angular velocity of the output gear ($\omega_{out}$) or that of the input gear ($\omega_{in}$), the equation can be rearranged as follows:

$$\omega_{in} = \frac{N_{out}}{N_{in}} \cdot \omega_{out} \tag{7}$$

Equation 7 allows for the determination of the angular velocity of either gear, given the number of teeth and the angular velocity of the other gear. In our particular scenario, where the number of teeth is identical across gears, an angular velocity counter-balance is achieved concerning the sides of the Rockerbot wheels allowing better stability concerning the irregular ground as highlighted by the test shown in Fig. 4b.

## Sensors

Concerning perceptual capabilities, Rockerbot is equipped with a 32-plane LiDAR, supplemented by a 1-plane laser scan for crop mapping. The primary source of odometric information is derived from an Intel RealSense feature-based camera, which offers superior adaptability to changes in vegetation compared to approaches based on point clouds. Furthermore, the robot incorporates an OAK-D Pro camera, complete with a neural inference chip. This setup enables real-time object detection during navigation and facilitates the distribution of computational load.

## Navigation method

The primary objective is to equip the robot with the ability to independently identify and follow crop rows. A crucial aspect of this process involves the robot's capability to detect the end of a row and subsequently execute a complete turn to continue its navigation in the next row. The navigation process is thus bifurcated into two distinct stages: row navigation and turning. The transition between these stages is facilitated by an end-of-row detector.

Our navigation method involves an inline process that partitions the surrounding point cloud of plants into two distinct groups through single-plane 2D clustering. These clusters are defined in real time, and we use the RANSAC algorithm to find the best-fitting line for each group. To ensure stability and address sudden changes in line slopes during the RANSAC convergence process, we use a sliding window of size 10, which includes a discount factor in the row direction.

With a well-defined line direction providing a local obstacle-free pathway, we calculate a series of control inputs to determine the next action, which could be either moving forward or retreating, depending on the situation. When navigation is active, a subprocess works to determine if the end of the maize row is approaching. If it is, a turning point is calculated based on the left or right direction, as indicated by the predefined path.

The turn is executed using the Nav2 framework, which considers a tuned cost map of the environment collected in real time during navigation. We retrieve the occupancy grid map with the help of a single-plane scan for close-range distances, and a multi-plane LiDAR for longer distances. The multi-plane LiDAR is preprocessed to merge a collection of planes slightly above the ground onto the same hypothetical plane. For computational efficiency, the ground is detected and removed.

## Watering procedure

Rockerbot possesses the capability to detect nearby plants during its navigation and administer a liquid solution to them. This functionality is facilitated by the use of a mono-plane laser-scan sensor. Employing a predetermined threshold, we group the lateral laser points to ascertain the presence or absence of plants. Subsequently, the watering system is activated to irrigate the identified plants. It's worth noting that while the system was initially designed for water, it can also be adapted for the dispensing of fertilizers,

pesticides, herbicides, or any other liquid solutions required to enhance crop quality in a maize field.

## Object detection

Rockerbot is equipped with the OAK-D Pro camera, which enables efficient object detection through dedicated on-board neural network serialization and deployment capabilities. Unlike other affordable commercial RGB-D cameras like the Intel RealSense, which necessitates off-board computation, the OAK-D Pro comes with built-in memory. This memory is specifically engineered to house a compact deep learning model in inference mode. This feature allows for quicker computations on its integrated chip and more efficient distribution of the robot's computational load. We have deployed a fine-tuned YOLOv8 medium-size model (Redmon et al., 2016) to distinguish between deers and humans.

To mitigate the possibility of misclassifications at run-time, which may not have been avoidable during training time, we implemented a dynamic sliding prediction FIFO (First-In-First-Out) buffer with a predefined size of 10 predictions. If the majority of predictions within this buffer belong to the same class, the system issues an alert with the corresponding class-specific signal.

The adopted YOLO settings for training encompass a comprehensive set of data augmentation techniques aimed at enhancing the robustness and diversity of the training dataset, composed by us of 23, 850 images. Firstly, an "auto-orient" approach is applied, ensuring that objects in the images are correctly oriented, thus minimizing potential biases associated with object orientations. The images are then resized to a uniform $416 \times 416$ resolution using a "center crop" strategy, which maintains the most informative region while eliminating unnecessary background information. Contrast stretching is employed to further augment the dataset, enhancing the visibility of objects and patterns in the images.

Horizontal and vertical flipping is introduced as part of the data augmentation pipeline, expanding the dataset by creating mirrored versions of the original images. Additionally, rotations of 90 degrees in both clockwise and counter-clockwise directions, as well as flipping images upside down, are applied to introduce variations in object orientations. To simulate real-world scenarios and introduce randomness, rotations within a range of –45 to +45 degrees are incorporated.

Furthermore, a controlled degree of variability is introduced through small random rotations, up to ±15 degrees, in both horizontal and vertical directions. These settings collectively contribute to a training dataset that is more comprehensive, diverse, and representative of real-world conditions, ultimately enhancing the performance

and generalization capabilities of the YOLO object detection model.

## RESULTS

### Kinematics

When assessing the skid-steering robot's performance, our initial validation test centered on its steering capabilities, specifically its ability to execute in-place turns. Our observations revealed a strong correlation between this ability and the robot's wheelbase dimension. To evaluate this behavior, we conducted a series of experiments in a controlled, level environment. Throughout these tests, we maintained a constant wheel separation (the distance between the left and right wheels) while varying the robot's wheelbase (the distance between its front and rear axles). We tested three different robot models with wheelbases of $0.15 m$, $0.32 m$, and $0.41 m$.

The results unequivocally demonstrated that the size of the robot's wheelbase had a significant impact on its in-place turning capabilities. A larger wheelbase led to a diminished capacity for the robot to execute in-place turns effectively. Consequently, we faced a decision between opting for a shorter wheelbase, which improved turning capabilities and choosing a longer one that ensured greater overall stability. Ultimately, for the final robot design, we settled on a wheelbase of $0.32 m$ to strike a balance between enhanced turning performance and overall stability.

### Suspensions

A comprehensive validation process was undertaken to assess the efficacy of the robot's suspension mechanism. Initially, simulation tests were performed in Gazebo ROS2, where the robot navigated through a simulated flat terrain with strategically placed bumps to engage only the right front and rear wheels. Subsequently, real-world validation tests were conducted to corroborate the simulation results and evaluate the practical performance of the suspension system. A meticulous methodology was employed to ensure precise replication of simulated conditions, guaranteeing accuracy and consistency in the evaluation process. The test track was accurately designed to mirror the simulated environment, facilitating an accurate assessment of real-world scenarios. The primary evaluation metric utilized was the robot's pitch angle profile, enabling a comparative analysis between active suspension and immobilized scenarios.

In both simulated and real-world environments, the robot's suspension mechanism demonstrated significant effectiveness in mitigating pitch angles when encountering bumps. Simulation results showcased a peak-to-peak pitch

angle reduction from 25.61 to 12.33 with an active suspension system, marking a notable 51.8% improvement compared to immobilized suspension. Real-world testing corroborated these findings, demonstrating consistent reductions in pitch angles with the suspension system enabled. Specifically, pitch angles decreased from

29.76 to 18.63, indicating a substantial 38.4% improvement in pitch angle mitigation. These results, illustrated in Fig. 4b, underscore the robustness and efficacy of the robot's suspension mechanism in real-world scenarios, validating its practical utility and performance.

### Odometry

The critical element essential for enabling autonomous navigation is the provision of reliable odometry data to guide the robot. Traditionally, this data is calculated using wheel encoders. However, due to the significant wheel slippage experienced in rugged terrains, exacerbated by the inherent characteristics of our kinematic system, we have incorporated an additional sensor – a visual odometry camera (specifically, the Intel T265).

To assess the performance of both systems, we recorded odometry data from both the wheel encoders and the camera, comparing them against the data obtained from a high-precision motion capture system. Our evaluation involved computing the Absolute Position Error (APE) between the respective trajectories. The resulting Root Mean Squared Error (RMSE) for the APE is presented in Table 1, underscoring the necessity of an external odometry source, such as the T265 camera, to mitigate the substantial errors associated with encoder-based odometry in a skid-steering robot.

**Table 1:** RMSE error in meters of the T265 and wheel encoder concerning the OptiTrack trajectory

| Method | RMSE |
| --- | --- |
| Encoder odometry T265 | 2.432022 |
| odometry | 0.596588 |

### Object detection

**Table 2:** Average precision (AP) by class: deer, human, and all

| | Validation | Testing |
| --- | --- | --- |
| all | 81% | 87% |
| deer | 88% | 90% |
| human | 74% | 84% |

The performance of the custom-trained YOLO model demonstrated effectiveness, as evidenced by the results presented. In Table 2, it can be observed that the model efficiently distinguished between deers and humans, achieving a higher Average Precision on the Testing Set

compared to the Validation Set used for hyper-parameter adjustment.

This implies that the model avoided overfitting the training data, making it a dependable option for real-world usage. Furthermore, the high metric values in Table 3 emphasize the model's efficacy on the dataset.

**Table 3:** Deployment and performance evaluation of the proposed fine-tuned YOLO model

| | mAP | Precision | Recall |
| --- | --- | --- | --- |
| Overall | 81.3% | 84.1% | 74.4% |

As depicted in Table 2, the testing set exhibited a higher mean Average Precision (mAP) score compared to the validation set, indicating the efficacy of fine-tuning without encountering overfitting issues. By delving into specific categories, particularly considering the balanced distribution of deers and humans in the training set, it becomes apparent from the data that the model became more adept at distinguishing between a deer and a human. This observation aligns with intuition, as deers typically maintain a consistent appearance across different habitats, whereas humans exhibit greater physical variability. This qualitative understanding elucidates why the mAP for humans is 84% and for deers is 90%. Nonetheless, both results are deemed excellent from a machine learning perspective on classification, thereby ensuring sufficient reliability for practical deployment.

The overall mAP of 81.3% reflects the model's comprehensive performance across all categories. This metric encapsulates both precision and recall, providing a holistic measure of the model's ability to correctly classify instances across various classes. The precision of 84.1% indicates the proportion of correctly identified instances among all instances classified as positive, highlighting the model's ability to minimize false positives. Conversely, the recall of 74.4% signifies the proportion of correctly identified instances among all actual positive instances, indicating the model's capacity to capture relevant instances without overlooking them. The balance between precision and recall is crucial in assessing the model's effectiveness in real-world scenarios, where both minimizing false positives and false negatives are essential for reliable decision- making. Therefore, the combination of these metrics offers valuable insights into the model's overall performance and its suitability for practical deployment in classification tasks.

## DISCUSSION

The results presented provide valuable insights into the design and performance of Rockerbot.

In terms of kinematics, the findings highlight the trade-off between turning capabilities and overall stability in the

context of the robot's wheelbase dimension. The decision to opt for a wheelbase of 0.32m represents a compromise between these two critical factors. This suggests that future designs might benefit from mechanisms that allow for adjustable wheelbase dimensions, enabling the robot to adapt to different operational requirements.

The research findings highlight the critical role of an active suspension system in augmenting the performance of robots, particularly in managing pitch angles. Both simulated and real-world tests demonstrated substantial enhancements, affirming the necessity of integrating such systems into robot designs. Further investigations could delve into the effects of varying suspension designs and configurations on overall robot performance, offering avenues for future research and development.

The odometry results highlight the challenges associated with obtaining reliable data in rugged terrains due to wheel slippage. The incorporation of a visual odometry camera (Intel T265) proved effective in mitigating these issues. This suggests that multi-modal sensor fusion, combining data from different types of sensors, could be a promising approach for improving odometry in skid-steering robots.

The performance of the custom-trained YOLO model in object detection tasks demonstrates the potential of deep learning techniques in enhancing the robot's autonomous navigation capabilities. The model's ability to generalize well to unseen data indicates its robustness and reliability, making it a promising choice for real-world deployment. Future research could explore the application of similar models to other object detection tasks, as well as the integration of these models into the robot's navigation system.

As future directions, enhancing the rotational curvature within a skid-steering model by advancing independent turning wheels offers a promising direction for future investigation. This endeavor entails refining kinematics to achieve the agility and precision observed in contemporary tractors. Additionally, there is a required emphasis on radar

odometry, which represents a forefront technology in agriculture. Its robustness in adverse weather conditions, despite the RTK-DGPS, provides unmatched reliability for navigation (Frosi et al., 2023) and localization tasks (Usuelli et al., 2023). The integration of radar-based sensing systems holds significant potential for augmenting autonomous operations, especially in demanding environments such as maize fields.

In conclusion, the results presented provide a strong foundation for the ongoing development and refinement of skid-steering robots, with implications for their kinematics, suspension, odometry, and object detection capabilities. Future work in this area would do well to build on these

findings, exploring the potential of adjustable wheelbase dimensions, multi-modal sensor fusion, and deep learning techniques in enhancing the performance and versatility of these robots.

### Field Robot Event 2023

We have had the pleasure of deploying this research in the renowned annual international competition Field Robotics Event (FRE) in autonomous robotics agriculture. Despite successfully fine-tuning the autonomous navigation system and achieving highly positive results, we encountered a technical glitch on the day of the competition. A defect in the motor's encoders caused two out of the four wheels to become inoperative, which unfortunately hindered our participation in the navigation task. Nevertheless, Rockerbot managed to secure the third position in the Object Detection contest, thereby validating the superior quality of our research. As we look to the future, our goal is to further improve Rockerbot's overall system for next year FRE 2024.

## CONCLUSION

In this study, we detailed the creation and refinement of a compact agricultural robot designed for autonomous navigation and surveillance of crop fields. The design decisions were initially tested and validated in a simulated environment before being applied in real-world conditions, effectively bridging the gap between theoretical design and practical application. This work was showcased at the esteemed Field Robotics Event 2023 in Maribor (Slovenia) where our proposed system secured third place in the Object Detection task. Looking ahead, we plan to further enhance the capabilities of Rockerbot, building on the success of this research and pushing the boundaries of autonomous agricultural technology.

## REFERENCES

1. Bakker, T., Van Asselt, K., Bontsema, J., & Van Henten, E. J. (2010). Robotic weeding of a maize field based on navigation data of the tractor that performed the seeding. *IFAC Proceedings Volumes, 43*, 157–159.
2. Chen, J., Qiang, H., Xu, G., Liu, X., Mo, R., & Huang, R. (2020). Extraction of navigation line based on improved

grayscale factor in corn field. *Cieñcia Rural,* 50, e20190699.

3. Cudrano, P., Mentasti, S., Locatelli, E., Nicolò, M., Portanti, S., Romito, A., Stavrakopoulos, S., Topal, G., Usuelli, M., Zinzani, M., & Matteucci, M. (2022). Detection and mapping of crop weeds and litter for agricultural robots. In 2022 *AEIT International Annual Conference (AEIT) (IEEE),* 1–6.

4. Diffenbaugh, N. S., Krupke, C. H., White, M. A., & Alexander, C. E. (2008). Global warming presents new challenges for maize pest management. *Environmental Research Letters, 3,* 044007.

5. Erenstein, O., Jaleta, M., Sonder, K., Mottaleb, K., & Prasanna, B. (2022). Global maize production, consumption and trade: trends and R&D implications. *Food Security: The Science, Sociology and Economics of Food Production and Access to Food, 14,* 1295–1319. https://doi.org/10.1007/s12571-022-01288-7

6. Fischler, M. A., & Bolles, R. C. (1981). Random sample consensus: a paradigm for model fitting with applications to image analysis and automated cartography. *Communications of the ACM* 24, 381–395.

7. Frosi, M., Usuelli, M., & Matteucci, M. (2023). Advancements in radar odometry. *arXiv preprint arXiv:2310.12729.*

8. Hiremath, S. A., Van Der Heijden, G. W., Van Evert, F. K., Stein, A., & Ter Braak, C. J. (2014). Laser range finder model for autonomous navigation of a robot in a maize field using a particle filter. *Computers and Electronics in Agriculture, 100,* 41–50.

9. Kozłowski, K., & Pazderski, D. (2004). Modeling and control of a 4-wheel skid-steering mobile robot. *International Journal of Applied Mathematics and Computer Science,* 14, 477–496.

10. Liu, L., Mei, T., Niu, R., Wang, J., Liu, Y., & Chu, S. (2016). Rbf-based monocular vision navigation for small vehicles in narrow space below maize canopy. *Applied Sciences,* 6, 182.

11. Redmon, J., Divvala, S., Girshick, R., & Farhadi, A. (2016). You only look once: Unified, real-time object detection. In *Proceedings of the IEEE conference on computer vision and pattern recognition.* 779–788.

12. Reiser, D., Miguel, G., Arellano, M. V., Griepentrog, H. W., & Paraforos, D. S. (2016). Crop row detection in maize for developing navigation algorithms under changing plant growth stages. In L. Reis, A. Moreira, P. Lima, L. Montano & V. Muñoz-Martinez (Eds.), *Robot 2015: Second Iberian Robotics Conference: Advances in Intelligent Systems and Computing,* vol 417 (pp 371–382). Springer, Cham.

13. Ritson, C. (2020). *Population Growth and Global Food Supplies.* In M. Rutland & A. Turner (Eds.), *Food Education and Food Technology in School Curricula. Contemporary Issues in Technology Education.* Springer, Cham. https://doi.org/10.1007/978-3-030-39339-7_17

14. Rubio, F., Valero, F., & Llopis-Albert, C. (2019). A review of mobile robots: Concepts, methods, theoretical framework, and applications. *International Journal of Advanced Robotic Systems,* 16(2). https://doi.org/10.1177/172988141983959

15. Sparrow, R. & Howard, M. (2021). Robots in agriculture: prospects, impacts, ethics, and policy. *Precision Agriculture, 22,* 818–833.

16. [Dataset] Statista (2021). Most grown crops in the world 2021. https://www.statista.com/ statistics/1003455/most-produced-crops-and-livestock-products -worldwide/

17. Usuelli, M., Frosi, M., Cudrano, P., Mentasti, S., & Matteucci, M. (2023). Radarlcd: Learnable radar-based loop closure detection pipeline. *arXiv preprint arXiv:2309.07094.*

18. Wang, T., Wu, Y., Liang, J., Han, C., Chen, J., & Zhao, Q. (2015). Analysis and experimental kinematics of a skid-steering wheeled robot based on a laser scanner sensor. *Sensors, 15,* 9681–9702.

19. Yang, S., Mei, S., & Zhang, Y. (2018). Detection of maize navigation centerline based on machine vision. *IFAC-PapersOnLine, 51,* 570–575.

# Rockerbot: Kinematika robotske platforme za pridelavo koruze

## IZVLEČEK

Pregledovanje in nadzor pridelka imata pomembno vlogo v sodobni kmetijski praksi, saj kmetom omogočata, da ocenijo stanje svojih njiv in na podlagih pravih informacij sprejemajo pravilne odločitve glede upravljanja s pridelki. Vendar so obstoječe metode pregledovanja pridelka pogosto računsko intenzivne, kar vodi do počasnih in dragih postopkov. Iz tega razloga obstaja zahteva po učinkovitejših in stroškovno dostopnejših pristopih za pregledovanje pridelkov, z namenom izboljšanja produktivnosti in trajnosti v kmetijstvu, kot tudi za reševanje težav glede pomanjkanja delovne sile. V tej raziskavi predstavljamo Rockerbot, nov kmetijski robot, ki je zasnovan kot kompaktni rover, sposoben krmariti in pregledovati koruzna polja v zgodnjih fazah rasti. Predstavljena tehnologija je bistvenega pomena za pravočasno prilagajanje spremembam, da se zagotovi optimalna pridelava pridelka. Delo ponuja celovit pregled korakov in odločitev, sprejetih v fazi razvoja strojne in programske opreme. Poglavje o strojni opremi je osredotočeno na dizajn robota, ki ga narekuje kinematika roverja, medtem ko poglavje o programski opremi opisuje naloge, ki jih lahko Rockerbot izvaja z uporabo mobilnega zaznavanja, kot so kartiranje, zaznavanje in odkrivanje.

Ključne besede: kmetijska robotika, pametno kmetijstvo, avtonomna navigacija, zalivanje, kartiranje